Hindawi Publishing Corporation
International Journal of Photoenergy
Volume 2013, Article ID 270389, 7 pages
http://dx.doi.org/10.1155/2013/270389

Research Article

Optical and Electrical Properties of the Different Magnetron Sputter Power 300°C Deposited Ga_2O_3-ZnO Thin Films and Applications in p-i-n α-Si:H Thin-Film Solar Cells

Fang-Hsing Wang,[1] Chia-Cheng Huang,[1] Cheng-Fu Yang,[2] and Hua-Tz Tzeng[1]

[1] *Department of Electrical Engineering, National Chung Hsing University, Taichung City, Taiwan*
[2] *Department of Chemical and Materials Engineering, National University of Kaohsiung, Kaohsiung 811, Taiwan*

Correspondence should be addressed to Cheng-Fu Yang; cfyang@nuk.edu.tw

Received 30 December 2012; Revised 20 February 2013; Accepted 21 February 2013

Academic Editor: Ho Chang

A compound of ZnO with 3 wt% Ga_2O_3 ($ZnO : Ga_2O_3 = 97 : 3$ in wt%, GZO) was sintered at 1400°C as a target. The GZO thin films were deposited on glass using a radio frequency magnetron sputtering system at 300°C by changing the deposition power from 50 W to 150 W. The effects of deposition power on the crystallization size, lattice constant (c), resistivity, carrier concentration, carrier mobility, and optical transmission rate of the GZO thin films were studied. The blue shift in the transmission spectrum of the GZO thin films was found to change with the variations of the carrier concentration because of the Burstein-Moss shifting effect. The variations in the optical band gap (E_g) value of the GZO thin films were evaluated from the plots of $(\alpha h\nu) = c(h\nu - E_G)^{1/2}$, revealing that the measured E_g value decreased with increasing deposition power. As compared with the results deposited at room temperature by Gong et al., (2010) the 300°C deposited GZO thin films had apparent blue shift in the transmission spectrum and larger E_g value. For the deposited GZO thin films, both the carrier concentration and mobility linearly decreased and the resistivity linearly increased with increasing deposition power. The prepared GZO thin films were also used as transparent electrodes to fabricate the amorphous silicon thin-film solar cells, and their properties were also measured.

1. Introduction

Tin-doped indium oxide (ITO) thin films are widely used as a transparent conducting oxide (TCO) electrode in optoelectronic devices, because the thin films have very low resistivity and high transmittance in the visible region. The radio frequency (RF 13.56 MHz) magnetron sputtering under different oxygen concentrations and deposition pressures was a good method to exhibit the good electrooptical characteristics of large area ITO thin films [1]. However, the price of indium is getting increased due to the high demand of ITO in the rapid development of flat panel displays (FPDs) industry. In addition, the toxic nature and high cost due to the scarcity of indium have led researchers to seek an alternative candidate for ITO. Zinc oxide (ZnO) is a novel II–VI compound n-type oxide semiconductor with a wurtzite crystal structure and with various electrical, optical, acoustic, and chemical properties because of its wide direct band gap (E_g) value of 3.37 eV at room temperature (RT) [2]. Because of the good properties of thin films, n-type doped ZnO thin films could be used as a transparent electrode in optoelectronic applications such as solar cells and position sensitive detectors, and undoped ZnO thin films could be used as the active layer of transparent thin films transistor [3]. Alternatively, In_2O_3-doped ZnO [4], Al_2O_3-doped ZnO [5], and Ga_2O_3-doped ZnO [6–8] are also regarded as the ideal candidates for replacing ITO as TCO electrodes owing to their promising optical and electrical properties as well as their low cost, nontoxicity, and long-term environmental stability.

Many researchers have reported about the Ga_2O_3-doped ZnO thin films according to a different doping concentration of Ga_2O_3 [9]. The highly conductive and transparent Ga_2O_3-doped ZnO thin films had been coated at high growth

rates by radio frequency magnetron sputtering [10]. The thin films processed at room temperature on soda lime glass substrates using a ceramic Ga_2O_3-doped ZnO target and a low resistivity of 2.6×10^{-4} Ω cm were obtained [11]. However, there is a still controversy about optimized deposition power for the Ga_2O_3-doped ZnO thin films. In the present paper, a compound of ZnO with 3 wt% Ga_2O_3 ($ZnO : Ga_2O_3 = 97 : 3$ in wt%, GZO) was prepared by solid-state reaction method. RF magnetron sputtering was developed in order to study the effects of different deposition powers on the physical and electrical properties of the GZO thin films. For that, the GZO thin films were deposited on glass substrates at 300°C by changing deposition power from 50 W to 150 W. We would show that the deposition power played an important role in nucleation, relatively diffraction intensity of orientations, lattice constant, strain, crystalline size, and optical E_g value of the GZO thin films. In the past, GZO thin films were used as the electrodes of the small area solar cells, produced in a modified single chamber reactor, and the fabricated solar cells exhibited very good electrical characteristics with a conversion efficiency exceeding 9% [12]. For that, the GZO thin films deposited under different deposition powers were also used as the transparent electrodes of the α-Si thin-film solar cells, and the current-voltage characteristics were measured to determine the effects that the deposition power of the GZO thin films had on the fabricated α-Si solar cells.

2. Experimental

ZnO (99.999% purity) and Ga_2O_3 (99.99% purity) powders were mixed with the formula of $ZnO : Ga_2O_3 = 97 : 3$ in wt% (GZO) and then ball milled for 5 h in deionized water. After being dried and ground, GZO powder was calcined at 1000°C for 2 h then ground again and mixed with polyvinyl alcohol (PVA) as a binder. The powder was uniaxially pressed into pellets of 3 mm thickness and 52 mm diameter using a steel die. After debindering, the pressed targets were sintered at different temperatures. We had found that at 1400°C was the optimal temperature to prepare the ceramic targets because the GZO ceramics sintered 1400°C had the densified and crystallization structure. The GZO thin films were deposited on 33 mm × 33 mm × 2 mm Corning 1737 glass substrates using an RF sputtering system. Before the deposition process was started, the base chamber pressure was pumped to 5×10^{-6} Torr (detected by using MKS Baratron gauge) and the substrate temperature was kept at 300°C, then the deposition pressure was controlled at 5×10^{-3} Torr. During the deposition process, only argon was introduced in the chamber, the flow rate of pure argon (99.999%) was 20 sccm, and the GZO thin films were deposited at different deposition powers (50 W~150 W). Film thickness was measured and surface morphology was observed by field emission scanning electron microscopy (FESEM), and the deposition rate was calculated from the measured thickness. By controlling the deposition time, a thickness of about 330 nm was attained for all GZO thin films. While the crystalline structure of the GZO thin films was identified by X-ray diffraction (XRD) patterns, the electrical resistivity was measured using a four-point probe, and the Hall-effect coefficient was measured using a Bio-Rad Hall setup. The optical transmission spectrum was recorded using a Hitachi U-3300 UV-Vis spectrophotometer in the 300–800 nm wavelength range. The current-voltage characteristic of the fabricated solar cells was measured under an illumination intensity of 300 mW/cm^2 and an AM 1.5 G spectrum.

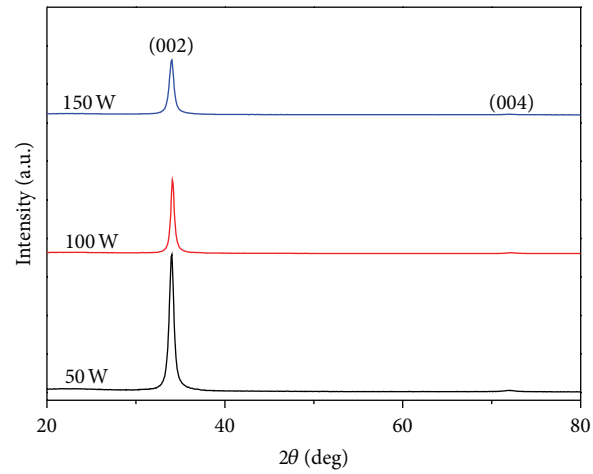

Figure 1: XRD patterns of the GZO thin films as a function of deposition power.

3. Results and Discussion

XRD patterns of the GZO thin films as a function of deposition power were shown in Figure 1, and all the GZO thin films exhibited the (002) peak. The (002) peaks of the GZO thin films prepared with deposition power = 50 W, 100 W, and 150 W were situated at $2\theta = 34.18°$, $34.11°$, and $34.04°$, respectively. The lattice constant c was calculated by using the 2θ value and the results were shown in Figure 2. The calculated lattice constant (c) was 0.5243, 0.5253, and 0.5262 for deposition power = 50 W, 100 W, and 150 W, respectively. All the lattice constants c of the GZO thin films in Figure 2 being smaller than that of the ZnO thin films are considerable, because the radius of Ga^{3+} ions (62 pm) are smaller than that of Zn^{2+} ions (72 pm).

As Figure 2 shows, the full width at half maximum (FWHM) values for the (002) peak of the GZO thin films is 0.389, 0.481, and 0.628 for deposition power = 50 W, 100 W, and 150 W, respectively. The relative diffraction intensity of (002) peak decreased as the deposition power increased, as indicated by the XRD patterns shown in Figure 1. These results suggest that GZO thin films deposited at lower power have the better crystalline structure. This is because larger deposition power is used to deposit the GZO thin films, GZO particles can have larger active energy, and the resputtering effect increased. For that, the number of thin film defects increases and the crystallization of the GZO thin films is inhibited, and then their crystallization of the GZO thin films is degenerated and the FWHM value increases. However, the variations of crystallization sizes are dependent on deposition power and are not easily calculated from the surface observation. We will illustrate the variations of grain sizes from

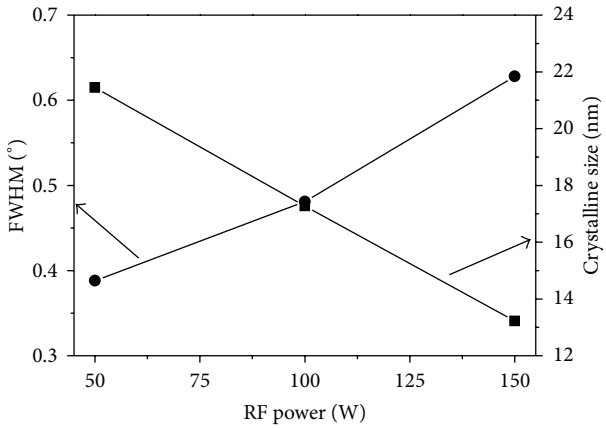

Figure 2: FWHM value and crystalline size of the GZO thin films as a function of deposition power.

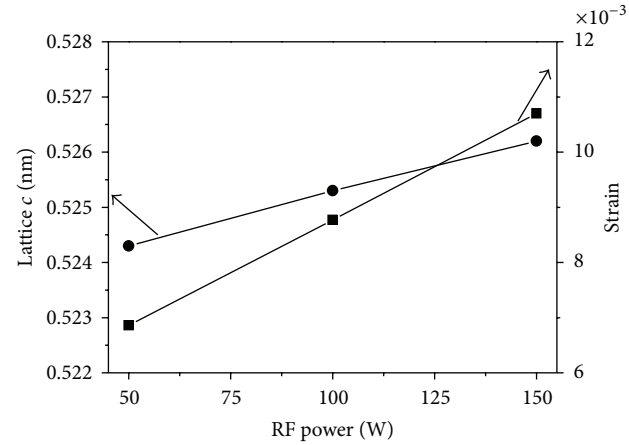

Figure 3: Lattice constant (c) and strain of the GZO thin films as a function of deposition power.

the XRD patterns and (1) [13], and the results are also shown in Figure 2.

$$D = \frac{(0.9\lambda)}{(\beta \cos\theta)}. \quad (1)$$

As Figure 2 shows, the crystallization size decreased with increasing deposition power. This is caused by the fact that as the deposition power increases, the deposition rate of the GZO thin films increases, and the chance for growth of the GZO crystallization size decreases.

Thin films always induce the internal stress, which might be misleading in determining the lattice parameters from one reflection when the thin films are under stress. We would also show that the deposition power has large influence on the strain of the GZO thin films. The relationships between lattice strain (η) and full width at FWHM (β) value can be expressed as (2) [14]

$$\frac{\beta \cos\theta}{\lambda} = \frac{2\eta \sin\theta}{\lambda} + \frac{1}{d}, \quad (2)$$

where θ is a Bragg's angle, λ is wavelength of X-ray, and d is crystallization size. For a XRD profile with more than 2 diffraction peaks, the 2η and $1/d$ could be separately obtained by calculating the slope and intercept of profile of $\sin\theta/\lambda$ versus $\beta\cos\theta/\lambda$. As Figure 3 shows, the lattice constant (c) linearly increased with increasing deposition power. The strain revealed a minimum value at RF deposition power = 50 W and then linearly increased as the deposition power increased. The phenomena are believed to be caused by the variations of mainly crystalline orientations, as shown in Figure 1.

In the past, determination of the optical E_g value was often necessary to develop the electronic band structure of a thin-film material. However, using extrapolation methods, the E_g value of the thin films can be determined from the absorption edge for direct interband transition, which can be calculated using (2) as

$$(\alpha h\nu) = c\left(h\nu - E_g\right)^{1/2}, \quad (3)$$

where α is the optical absorption coefficient, c is the constant for direct transition, h is Planck's constant, and ν is the frequency of the incident photon [15].

Figure 4(a) shows the transmission rate of the GZO thin films, with deposition power as the parameter. The optical transmission rates at 400–700 nm was more than 78% for all the GZO thin films, regardless of deposition power. As the deposition power increased, the optical band edge was shifted to a longer wavelength. Figure 4(b) plots $(\alpha h\nu)^2$ against $h\nu$ (energy) in accordance with (3), and the E_g values can be found by extrapolating a straight line at $(\alpha h\nu) = 0$. The calculated E_g values of the GZO thin films as a function of deposition power are also shown in Figure 4(b). The linear dependence of $(\alpha h\nu)$ on $h\nu$ indicates that the GZO thin films are direct transition-type semiconductors. As the deposition power increased from 50 W to 150 W, the E_g values decreased from 3.83 eV to 3.76 eV and the absorption edge was at around wavelength 370 nm (transmittance ratio over 60%). As compared with the results deposited at room temperature by Gong et al., the deposited GZO thin films had E_g values changed from 3.42 eV to 3.50 eV [6] and had absorption edge at around wavelength 400 nm. The 300°C deposited GZO thin films had larger E_g value and apparent blue-shift in the transmission spectrum. In the past, the GZO thin films were also deposited on the polyethylene naphthalate (PEN) substrates by RF magnetron sputtering at room temperature [16]. However, the FWHM values of the 300°C deposited GZO thin films developed in this study are smaller than those of [16], suggesting that the 300°C deposited GZO thin films have the better crystallization.

Many factors will affect the transmission spectrum of the GZO thin films. At first, the increase of the transmission ration in the optical band is caused by the increase in carrier density, as the GZO thin films have fewer defects. When the deposition temperature in this study is 300°C, the high deposition power can cause the GZO thin films to have the better crystallization. This is another reason to cause the GZO thin films in this study to have the higher transmittance ratio in the region of visible light. The results in Figure 4 suggest

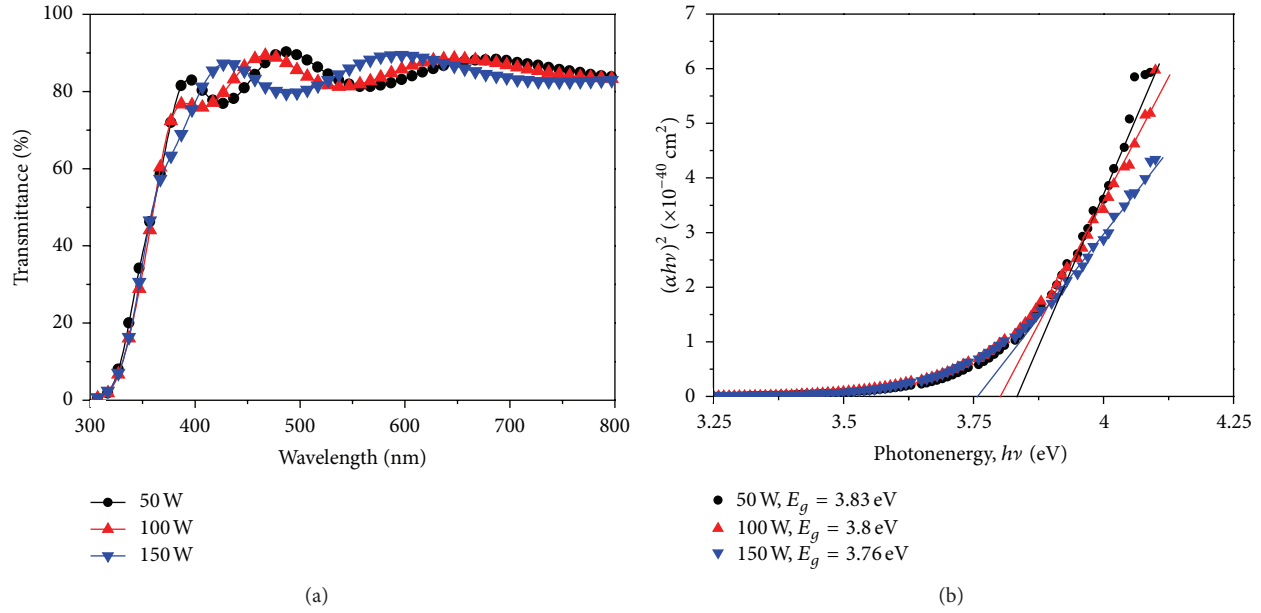

FIGURE 4: (a) Transmittance and (b) $(\alpha h\nu)^2$ versus $h\nu$-E_g plots of the GZO thin films as a function of deposition power.

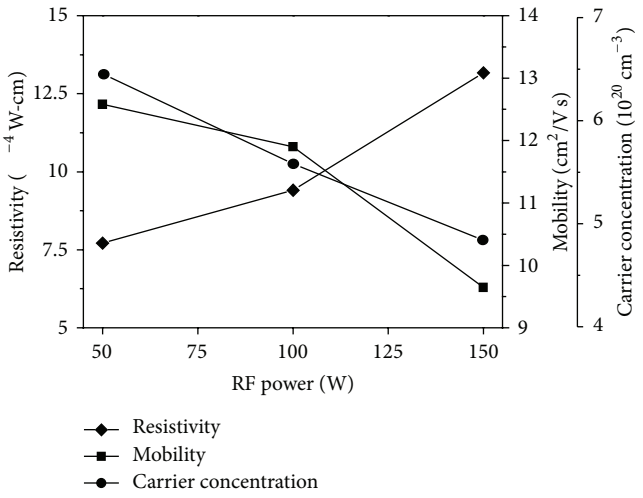

FIGURE 5: Resistivity (ρ), Hall mobility (μ), and carrier concentration (n) of the GZO thin films as a function of deposition power.

that the defects in the GZO thin films increase with increasing deposition power. However, the E_g value of Ga_2O_3 is 4.9 eV [17] and the E_g value of ZnO is about 3.37 eV. As Ga_2O_3 is added into the ZnO, the E_g values of the GZO thin films higher than those of the ZnO thin films are expected.

Figure 5 shows the dependence of electrical properties on deposition power of the GZO thin films. When plasma molecules are deposited on a glass substrate, many defects result and inhibit electron movement. As the different deposition powers are used during the deposition process, two factors are believed to cause the decreased carrier mobility of the GZO thin films. First, the larger deposition power provides more energy and thus enhances the motion of deposition atoms, which would increase the number of defects in the GZO thin films. Second, as the deposition power increases, the density of the GZO thin films decreases because of the increase in the defects, and that will cause the increase in the inhibiting of the barriers electron transportation [18]. A minimal resistivity of $7.71 \times 10^{-4}\ \Omega$ cm is obtained at a deposition power of 50 W; meanwhile, the carrier concentration has a maximum of 6.44×10^{20} cm^{-3} and the mobility has a maximum of 6.44 cm^2/V-s. The resistivity of the TCO thin films is proportional to the reciprocal of the product of carrier concentration N and mobility μ

$$\rho = \frac{1}{Ne\mu}. \tag{4}$$

Both the carrier concentration and the carrier mobility contribute to the conductivity. As Figure 5 shows, both the carrier concentration and carrier mobility of the GZO thin films decreased linearly with increasing deposition power and reached a minimum concentration and a minimum carrier mobility at 150 W. The minimum resistivity of the GZO thin films at a deposition power of 50 W is mainly caused by the carrier concentration and mobility being at their maximum.

As the deposition power rose, the absorption edge of the GZO thin films was blue shifted. This blue shift can be explained by the Burstein-Moss shift, a shift of the Fermi level into the conduction band, which enhances the optical E_g value by the energy, as follows [19, 20]:

$$\Delta E_g^{\mathrm{BM}} = \frac{\hbar^2 k_F^2}{2}\left(\frac{1}{m_e} + \frac{1}{m_h}\right) = \frac{\hbar^2 k_F^2}{2m_{vc}^*}, \tag{5}$$

where k_F stands for the Fermi wave vector and is given by $k_F = (3\pi^2 n_e)^{1/3}$, m_e is the effective mass of electrons in

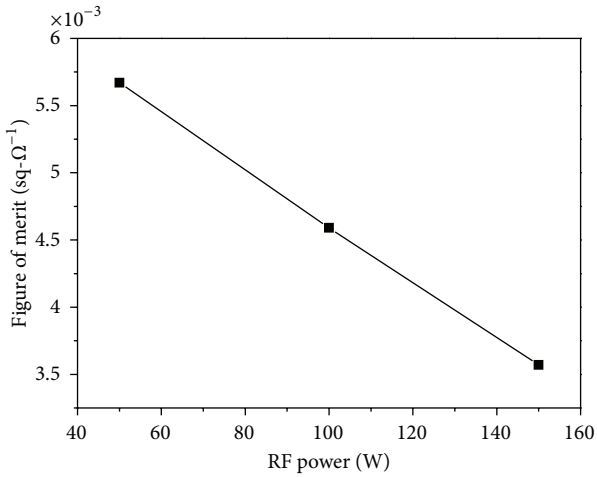

Figure 6: Figure of merit (FOM) of GZO thin films as a function of deposition power.

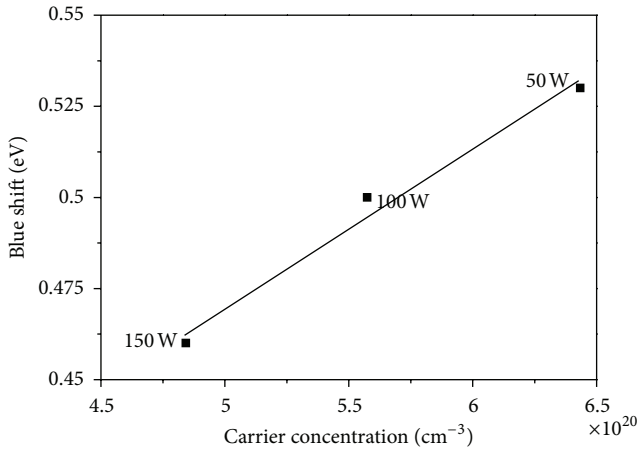

Figure 7: Blue shift of the GZO thin films as a function of carrier concentration.

the conduction band, and m_h is the effective mass of holes in the valence band, which can be simplified as m^*_{vc}, the reduced effective mass. ΔE_g value can be rewritten by inducing k_F for the carrier concentration n_e as

$$\Delta E_g^{\mathrm{BM}} = \frac{\hbar^2}{2m^*_{vc}}\left(3\pi^2 n_e\right)^{2/3}. \quad (6)$$

Equation (4) shows that the Burstein-Moss shift of the absorption edge to the shorter wavelength region is due to the increase in carrier concentration (n_e); this is proven by the result shown in Figure 6. When the wavelength is equal to 300 nm, the visible light absorbed by the thin films is due to a quantum phenomenon called band edge absorption. Burstein indicated that an increase of the Fermi level in the conduction band of a degenerated semiconductor leads to the energy band widening effect [9, 10].

For the application as transparent electrodes of solar cells, the films must have high electrical conductance and high optical transparency. A way for evaluating this compromise

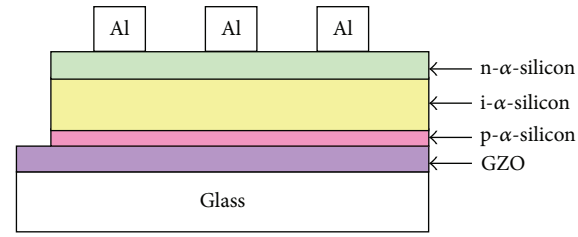

Figure 8: Structure of the superstrate p-i-n α-Si:H thin-film solar cells.

is by means of figure of merit (FOM). FOM defined by Haacke [21] is one of the important indexes for judging the effectiveness of the deposited thin films. FOM is defined by

$$\mathrm{FOM} = \frac{T^{10}}{R_s}, \quad (7)$$

where T is the average visible transmittance and R_S is the sheet resistance. Figure 7 exhibits the FOM of the GZO thin films prepared as a function of deposition power. The FOM value decreased with increasing deposition power and the highest FOM value of $5.67 \times 10^{-3}\ \Omega^{-1}$ was obtained at the sputtering power of 50 W. Those results prove that the 50 W is the optimal deposition power of the GZO thin films.

Superstrate p-i-n α-Si:H thin film solar cells were fabricated using a single-chamber plasma-enhanced chemical vapor deposition unit at 200°C. Figure 8 shows the structure of these solar cells, and no antireflective coatings were deposited on those devices. Figure 9 shows the measured current-voltage characteristics of the solar cells (substrate size $3.3 \times 3.3\ \mathrm{cm}^2$) under illumination. Table 1 lists the values of the open-circuit voltage (V_{oc}), short-circuit current density (J_{sc}), fill factor (F.F.), and efficiency (η) for the solar cells using the developed GZO thin films as the front transparent conductive thin films. The efficiency of the solar cells with the GZO thin films increased from 2.83% to 3.38% as deposition power decreased from 150 W to 50 W. The greater efficiency of the 50 W deposited GZO thin films is mainly ascribable to the fact that they have the larger E_g value, smaller strain, larger FOM value, and smaller resistivity, and those will cause the smaller short-circuit current density and larger open-circuit voltage.

4. Conclusions

The full width at half maximum (FWHM) values for the (002) peak of the GZO thin films were 0.389, 0.481, and 0.628 for deposition power = 50 W, 100 W, and 150 W. Because the 300°C deposited GZO thin films had the better crystallization, the transmittance ratios were higher than other studies. Also, the strain revealed a minimum value at deposition power = 50 W and then linearly increased as the deposition power increased. A minimal resistivity of $7.71 \times 10^{-4}\ \Omega$ cm was obtained at a deposition power of 50 W; meanwhile, the carrier concentration had a maximum of $6.44 \times 10^{20}\ \mathrm{cm}^{-3}$ and the mobility had a maximum of $6.44\ \mathrm{cm}^2$/V-s. As the deposition power increased from 50 W to 150 W,

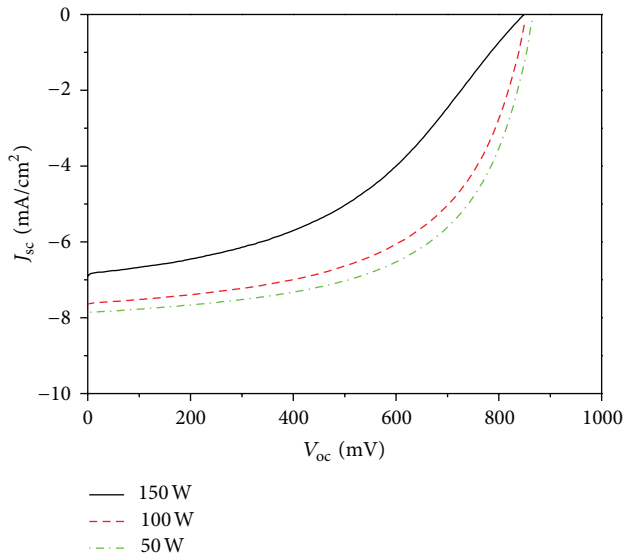

Figure 9: Current-voltage characteristics of the p-i-n α-Si:H thin-film solar cells under illumination.

Table 1: Values of open-circuit voltage (V_{oc}), short-circuit current density (J_{sc}), fill factor (F.F.), and efficiency (η) for solar cells with the different power-deposited GZO thin films.

Deposition power	V_{oc} (mV)	J_{sc} (mA/cm^2)	F.F.	η (%)
50 W	868	7.86	0.508	3.38
100 W	843	7.64	0.502	3.18
150 W	838	6.95	0.465	2.83

the calculated E_g values decreased from 3.83 eV to 3.76 eV, which were also higher than other studies. The GZO thin films having the larger E_g values were expected because the E_g value of the Ga_2O_3 thin films (4.9 eV) was larger than that of the ZnO thin films (3.35 eV). When the GZO thin films were used as the front transparent conductive thin films, the efficiencies of the α-Si thin-film solar cells increased from 2.83% to 3.38% as the deposition power decreased from 150 W to 50 W.

Acknowledgments

The financial support under Grants NSC 101-2221-E-005-065 and 99-2221-E-390-013-MY2 and the help of H.-T. Tzeng in the experimental process.

References

[1] I. Baia, M. Quintelab, L. Mendesa, P. Nunesa, and R. Martins, "Performances exhibited by large area ITO layers produced by r.f. magnetron sputtering," *Thin Solid Films*, vol. 337, no. 1-2, pp. 171–175, 1999.

[2] Ü. Özgür, I. Ya. Alivov, C. Liu et al., "A comprehensive review of ZnO materials and devices," *Journal of Applied Physics*, vol. 98, no. 4, Article ID 041301, 103 pages, 2005.

[3] E. Fortunato, A. Gonçalves, A. Pimentel et al., "Zinc oxide, a multifunctional material: from material to device applications," *Applied Physics A*, vol. 96, no. 1, pp. 197–205, 2009.

[4] R. Martins, P. Almeida, P. Barquinha et al., "Electron transport and optical characteristics in amorphous indium zinc oxide films," *Journal of Non-Crystalline Solids*, vol. 352, no. 9–20, pp. 1471–1474, 2006.

[5] F. H. Wang, H. P. Chang, C. C. Tseng, C. C. Huang, and H. W. Liu, "Influence of hydrogen plasma treatment on Al-doped ZnO thin films for amorphous silicon thin film solar cells," *Current Applied Physics*, vol. 11, supplement 1, pp. S12–S16, 2011.

[6] L. Gong, J. Lu, and Z. Ye, "Transparent and conductive Ga-doped ZnO films grown by RF magnetron sputtering on polycarbonate substrates," *Solar Energy Materials and Solar Cells*, vol. 94, no. 6, pp. 937–941, 2010.

[7] C. B. Yan, X. L. Chen, F. Wang et al., "Textured surface ZnO: B/(hydrogenated gallium-doped ZnO) and (hydrogenated gallium-doped ZnO)/ZnO:B transparent conductive oxide layers for Si-based thin film solar cells," *Thin Solid Films*, vol. 521, pp. 249–252, 2012.

[8] D. H. Lee, K. Kim, Y. S. Chun, S. Kim, and S. Y. Lee, "Substitution mechanism of Ga for Zn site depending on deposition temperature for transparent conducting oxides," *Current Applied Physics*, vol. 12, no. 6, pp. 1586–1590, 2012.

[9] S. Liang and X. Bi, "Structure, conductivity, and transparency of Ga-doped ZnO thin films arising from thickness contributions," *Journal of Applied Physics*, vol. 104, no. 11, Article ID 113533, 5 pages, 2008.

[10] S. Kim, W. I. Lee, E. H. Lee, S. K. Hwang, and C. Lee, "Dependence of the resistivity and the transmittance of sputter-deposited Ga-doped ZnO films on oxygen partial pressure and sputtering temperature," *Journal of Materials Science*, vol. 42, no. 13, pp. 4845–4849, 2007.

[11] V. Assunção, E. Fortunato, A. Marques et al., "Influence of the deposition pressure on the properties of transparent and conductive ZnO:Ga thin-film produced by r.f. sputtering at room temperature," *Thin Solid Films*, vol. 427, no. 1-2, pp. 401–405, 2003.

[12] R. Martins, L. Raniero, L. Pereira et al., "Nanostructured silicon and its application to solar cells, position sensors and thin film transistors," *Philosophical Magazine*, vol. 89, no. 28–30, pp. 2699–2721, 2009.

[13] L. V. Azaroff, *Element of X-Ray Crystallography*, McGraw-Hill, New York, NY, USA, 1968.

[14] W. Liu, G. Du, Y. Sun et al., "Al-doped ZnO thin films deposited by reactive frequency magnetron sputtering: H_2-induced property changes," *Thin Solid Films*, vol. 515, no. 5, pp. 3057–3060, 2007.

[15] N. Serpone, D. Lawless, and R. Khairutdinov, "Size effects on the photophysical properties of colloidal anatase TiO_2 particles: size quantization or direct transitions in this indirect semiconductor?" *Journal of Physical Chemistry*, vol. 99, no. 45, pp. 16646–16654, 1995.

[16] E. Fortunato, A. Gonçalves, A. Marques et al., "New developments in gallium doped zinc oxide deposited on polymeric substrates by RF magnetron sputtering," *Surface and Coatings Technology*, vol. 180-181, pp. 20–25, 2004.

[17] M. Orita, H. Ohta, M. Hirano, and H. Hosono, "Deep-ultraviolet transparent conductive ß-Ga_2O_3 thin films," *Applied Physics Letters*, vol. 77, no. 25, pp. 4166–4168, 2000.

[18] Y. Igasaki and H. Saito, "Substrate temperature dependence of electrical properties of ZnO:Al epitaxial films on sapphire (1210)," *Journal of Applied Physics*, vol. 69, no. 4, pp. 2190–2195, 1991.

[19] E. Burstein, "Anomalous optical absorption limit in InSb," *Physical Review*, vol. 93, no. 3, pp. 632–633, 1954.

[20] I. Hamberg, C. G. Granqvist, K. F. Berggren, B. E. Sernelius, and L. Engström, "Band-gap widening in heavily Sn-doped In_2O_3," *Physical Review B*, vol. 30, no. 6, pp. 3240–3249, 1984.

[21] G. Haacke, "New figure of merit for transparent conductors," *Journal of Applied Physics*, vol. 47, no. 9, pp. 4086–4089, 1976.